International Journal of Bifurcation and Chaos, Vol. 22, No. 10 (2012) 1250248 (8 pages)

DOI: 10.1142/S0218127412502483

THE EFFECT OF WEAK DISSIPATION IN TWO-DIMENSIONAL MAPPING

JULIANO A. DE OLIVEIRA* and EDSON D. LEONEL†
Departamento de Estatística, Matemática Aplicada e Computação,
Instituto de Geociências e Ciências, Exatas,
UNESP–Univ. Estadual Paulista, Av.24A, 1515,
Bela Vista, CEP: 13506-900 Rio Claro, SP, Brazil
**julianoantonio@gmail.com*
†*edleonel@rc.unesp.br*

Received March 28, 2011; Revised November 1, 2011

The influence of weak dissipation and its consequences in a two-dimensional mapping are studied. The mapping is parametrized by an exponent γ in one of the dynamical variables and by a parameter δ which denotes the amount of the dissipation. It is shown that for different values of γ the structure of the phase space of the nondissipative model is replaced by a large number of attractors. The approach to the attracting fixed point is characterized both analytically and numerically. The attracting fixed point exhibits a very complicated basin of attraction.

Keywords: Dissipation; attracting fixed point; basin of attraction.

1. Introduction

Studies of nonlinear two-dimensional mappings have been under consideration by many during the last decades [Lichtenberg & Lieberman, 1992; Zaslavsky, 1998]. Applications of this formalism can be used in the study of periodically corrugate waveguide [Leonel, 2007; Rabelo & Leonel, 2008; Virovlyansky & Zaslavsky, 2000; Smirnov *et al.*, 2001], channel flows [Luna-Acosta *et al.*, 2002; Zaslavsky, 2002], billiards [Leonel & Bunimovich, 2010; Berry, 1981], Fermi acceleration [Karlis *et al.*, 2006; Leonel *et al.*, 2004] and also for the study of magnetic field lines in toroidal plasma devices with reversed shear (like tokamaks) [Howard *et al.*, 1986; Saif *et al.*, 1998; Saif, 2000; Luna-Acosta *et al.*, 1996] and in suppression and production of Fermi acceleration [Ladeira & Leonel, 2010], among others.

A dynamical system generally has one or more control parameters. They can control the nonlinearity, and different characterizations can be made like measuring the Lyapunov exponents, finding the fixed points and obtaining a transition from integrability to nonintegrability. For the conservative case, i.e. when dissipative forces are absent, regular motions around the stable periodic orbits can be observed as well as Kolmogorov–Arnold–Moser (KAM) islands and invariant tori. The periodic orbits can be classified in two differents forms, such as [Lichtenberg & Lieberman, 1992; Feudel *et al.*, 1996; Feudel & Grebogi, 1997]: (i) primary islands are fixed points of period-1 and (ii) periodic orbits of period > 1. In the second case, the periodic orbits make up the largest regions of the regular behavior in the phase space and are surrounded by small islands of stability. These small islands have higher period and are secondary islands. Generally, the secondary orbits fill small regions of the phase space when compared with primary islands. Regions with chaotic motions can be observed too. Both motions can be illustrated in the phase space of these mappings exhibiting a large chaotic sea that eventually

surrounds KAM islands and is limited by a set of invariant tori [Lichtenberg & Lieberman, 1992]. The size of the chaotic sea is strongly influenced by the control parameters given that they control the nonlinearity.

The introduction of dissipation in a dynamical system destroys all structures of the phase space observed for a conservative model. Thus, it is possible to observe different asymptotic behaviors when the damping is varied. For instance, the effects of transient [Liberman & Tsang, 1985], attractive fixed points [Luck & Mehta, 1993], periodic orbits [Tavares & Leonel, 2008] and chaotic attractors [Tsang & Lieberman, 1984] can be considered. If a small dissipation is introduced in a conservative system, the periodic orbits turn into a finite number of periodic attractors. The number of attractors depends on the damping level and of the systems under consideration. The periodic orbits are converted into an attractor and such attractor exists even for large damping. Generally, in dynamical systems the number of periodic attractors are associated with the primary islands by 1/damping [Feudel & Grebogi, 1997]. This shows that if the damping tends to zero the number of periodic attractors tends to infinity. The association with the conservative system provides that primary islands correspond to a set of periodic orbits. For the secondary islands in some systems the number of attractors is less than the primary one [Feudel *et al.*, 1996; Feudel & Grebogi, 1997].

The description of dissipative dynamical systems is important for the study of the motion of a particle within fluid with gas [Leonel & McClintock, 2006; Leonel & Tavares, 2007], irreversibility in complex systems charge and energy transfer in quantum molecular systems [May & Kuhn, 2000], and even for describing dissipation in quantum mechanics [Castro Neto & Caldeira, 1991], for the investigation of basin size evolution between dissipative and conservative limits [Rech *et al.*, 2005], fractal dimension of the set of singularities for a scattering function [Seoane *et al.*, 2007], for the model of the finite bath [Rosa & Beims, 2008] and in the mechanical systems that consist of two rotors that possess a large number (3000+) of coexisting periodic attractors [Feudel *et al.*, 1998] and many others.

In this paper, we consider the introduction of dissipation in a family of two-dimensional mapping [de Oliveira *et al.*, 2010]. The dissipation is considered such that for $\delta = 0$ the system is conservative. Thus, the dissipation destroys the mixed structure of the phase space and creates a large number of attractors. Each one of the attractors has a complicated basin of attraction. The convergence to the attractor is shown to be exponential and was characterized both analytically and numerically.

The paper is organized as follows. In Sec. 2 we present the model and discuss the variables and control parameters used. Section 3 is devoted to present our results. Finally, in Sec. 4, we draw our concluding remarks.

2. Definition of the Problem and the Mapping

In this paper, we consider a family of dissipative two-dimensional mapping given by

$$T : \begin{cases} x_{n+1} = \left[x_n + \dfrac{a}{y_{n+1}^{\gamma}} \right] \mod 1 \\ y_{n+1} = |(1-\delta)y_n - b\sin(2\pi x_n)|, \end{cases} \tag{1}$$

where a, b, δ and γ are the control parameters. Some of the motivations for considering this form of the mapping comes from [de Oliveira *et al.*, 2010] where a careful study of the conservative case was carried out and critical exponents from a phase transition from integrability to nonintegrability were obtained. Since the present form was not yet discussed in the literature, it is important to understand the laws which describe the convergence to the attractors and some of their characteristics. The determinant of the Jacobian matrix is $\mathrm{Det}\,\mathrm{J} = (1-\delta)\mathrm{sign}[(1-\delta)y_n - b\sin(2\pi x_n)]$ where $\mathrm{sign}(u) = 1$ if $u > 0$ and $\mathrm{sign}(u) = -1$ if $u < 0$. One can see that if $\delta = 0$ the conservative system is recovered.

The coordinates of the period-1 fixed points of the mapping (1) can be obtained by matching the following conditions: $y_{n+1} = y_n = y$ and $x_{n+1} = x_n = x + m$, where $m = 1, 2, 3, \ldots$. After some algebra, we obtain the fixed points as

$$(x, y) = \left(\frac{1}{2\pi} \arcsin \left[\frac{-\delta}{b} \left(\frac{2}{m} \right)^{1/\gamma} \right], \left(\frac{2}{m} \right)^{1/\gamma} \right), \tag{2}$$

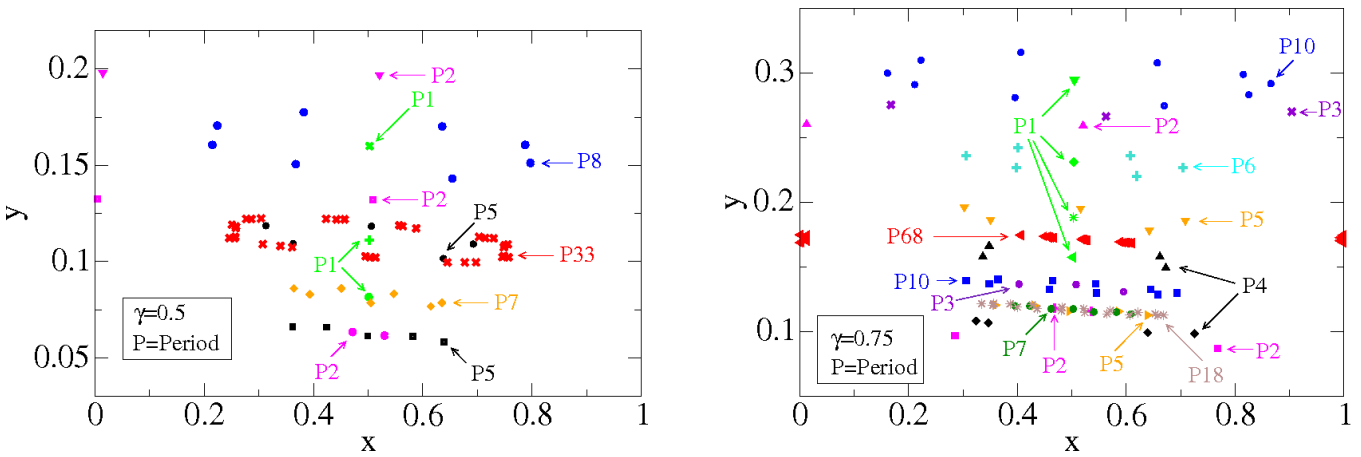

Fig. 1. Attracting fixed point observed for the mapping (1) for the control parameters, $a = 2$, $b = 10^{-2}$, $\delta = 10^{-3}$, and (a) $\gamma = 1/2$, (b) $\gamma = 3/4$.

which are unstable and

$$(x, y) = \left(\frac{1}{2\pi} \left\{ \pi - \arcsin \left[\frac{-\delta}{b} \left(\frac{2}{m} \right)^{1/\gamma} \right] \right\}, \left(\frac{2}{m} \right)^{1/\gamma} \right), \tag{3}$$

that can be stable for specific set of control parameters.

The attracting fixed point with period larger than 1 was obtained numerically. Figure 1 shows some of the attractors and their period obtained for the control parameters $a = 2$, $b = 10^{-2}$, $\delta = 10^{-3}$ in (a) $\gamma = 1/2$ and (b) $\gamma = 3/4$. Each initial condition was evolved up to 10^7 iterations as an attempt to avoid the effects of the transient. The range of initial conditions were $x \in (0, 1]$ and $y = [5 \times 10^{-3}, 0.22]$ for Fig. 1(a) while $y = [5 \times 10^{-4}, 0.33]$ for Fig. 1(b). The highest period accounted was (a) 33 and (b) 68.

3. Numerical Results

We begin discussing the convergence to the attractors. To investigate the convergence to an attracting fixed point we define a set of initial conditions along the basin of attraction of an attractor and allow them to evolve in time. In order to check whether the initial condition has reached the fixed point, we define a convergence criterion to check the asymptotic approximation of the attractive fixed point. It consists of obtaining the distance of the orbit from a fixed point. We define a distance r and evolve the initial conditions. If an orbit is sufficiently close to an attracting fixed point, considering a distance lower than r, then the number of iterations spent to reach such a condition is kept and a new initial condition is started. The average number of iterations for an ensemble of M initial conditions is obtained as

$$\overline{n} = \frac{1}{M} \sum_{i=1}^{M} n_i. \tag{4}$$

A plot of $r \times \overline{n}$ shows how the average behavior of the ensemble of initial conditions evolve to the fixed point. The distance from the fixed point is obtained as $r = \sqrt{(x_n - x_f)^2 + (y_n - y_f)^2}$ where (x_f, y_f) are the coordinates of the fixed point. Figure 2(a) illustrates a typical behavior of $r \times \overline{n}$. Each curve corresponds to a different value of δ. The average was performed using $M = 500$ different initial conditions for the control parameters $a = 2$, $b = 10^{-2}$, $\gamma = 1/2$. The curves illustrated in such a figure are fitted by $r_n = r_0 \exp(An)$. For $\delta = 10^{-4}$, we obtained $r_0 = 5.1(6) \times 10^{-2}$ and $A = -1.0001(1) \times 10^{-5}$. Using $\delta = 2 \times 10^{-5}$ it was found $r_0 = 0.5(2) \times 10^{-2}$ and $A = -5.002(2) \times 10^{-5}$. These results allow us to conclude that the trajectories exponentially approach a fixed point. Figure 2(b) illustrates the behavior of $\overline{n} \times \delta$. This behavior can be described as

$$\overline{n} \propto \delta^{\mu}. \tag{5}$$

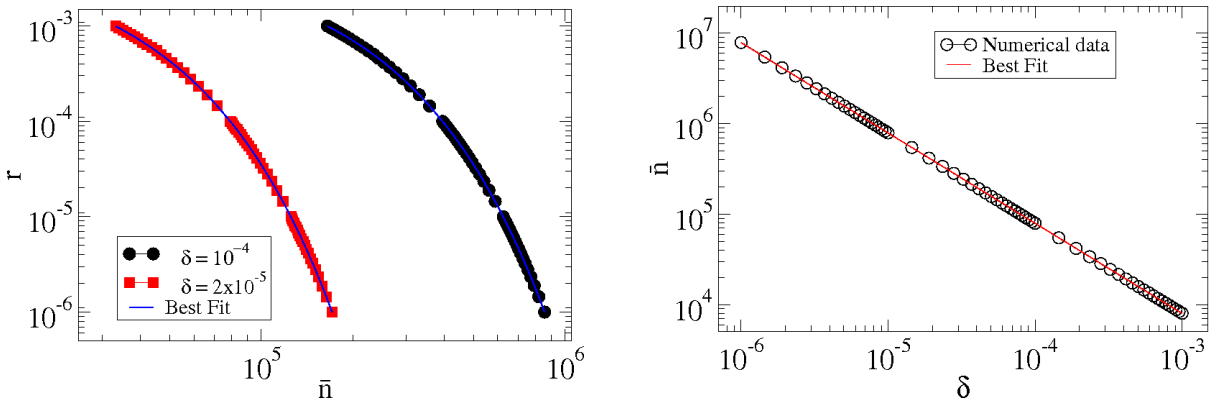

Fig. 2. (a) Plot of $r \times \overline{n}$, (b) plot of $\overline{n} \times \delta$.

A power law fit shown in Fig. 2(b) gives $\mu = -0.9980(1) \cong -1$. One can see that in the limit of $\delta \to 0$, Eq. (5) yields $\overline{n} \to \infty$. Of course, $\overline{n} \to \infty$ implies that the convergence to the attracting fixed point has not occurred, as it was expected to be observed in the nondissipative case. Specific discussion for the problem of the one-dimensional Fermi accelerator model under the presence of frictional force can be found in [Leonel & McClintock, 2006; Leonel & Tavares, 2007]. The power-law scaling of the number of attractors is fairly common, but not general, since the scaling can be also exponential sometimes.

Let us now give an analytical argument for the exponential approach to the fixed points. We consider a large value of y as the initial condition. We iterate the second equation of the mapping (1) and obtain

$$\begin{aligned} y_1 &= |(1-\delta)y_0 - b\sin(2\pi x_0)|, \\ y_2 &= |(1-\delta)^2 y_0 - b[(1-\delta)\sin(2\pi x_0) \\ &\quad + \sin(2\pi x_1)]|, \\ y_3 &= |(1-\delta)^3 y_0 - b[(1-\delta)^2\sin(2\pi x_0) \\ &\quad + (1-\delta)\sin(2\pi x_1) + \sin(2\pi x_2)]|. \end{aligned} \tag{6}$$

A general expression can be written as

$$y_n = (1-\delta)^n y_0 - b\sum_{i=1}^{n}(1-\delta)^{n-i}\sin(2\pi x_{i-1}). \tag{7}$$

Let us now consider specific limits for the parameter δ and initial condition y_0. Given that we are considering small dissipation, we assume that $0 < \delta \ll 1$. Additionally we use a large y_0 when compared to the length of b, typically $y_0 = 10^3 b$. Moreover given the periodicity of the sine function, the second term in Eq. (7) after the equality can be neglected as it contributes just a small oscillation around the average decay. Expanding the first term in powers of n, we obtain

$$y_n \simeq y_0\left[1 + \sum_{j=1}^{k}\frac{1}{j!}[\ln(1-\delta)]^j n^j\right]. \tag{8}$$

The term $\ln(1-\delta)$ inside of the brackets can be written as

$$\ln(1-\delta) \simeq -\delta - \frac{\delta^2}{2} - \frac{\delta^3}{3} - \frac{\delta^4}{4} + \cdots. \tag{9}$$

Considering that δ is sufficiently small, we keep only the first term in Eq. (9). Substituting this result in Eq. (8), we recover the definition of the exponential, as follows

$$y_n = y_0\, e^{-\delta n}. \tag{10}$$

Figure 3(a) shows the behavior of y as a function of n. One can see that an exponential decay of y with n is observed. The control parameters used in the construction of Fig. 3 were $a = 2$, $b = 10^{-2}$, $\delta = 5 \times 10^{-4}$ and $\gamma = 1/2$. We show in Fig. 3(a) that using the initial condition $x_0 = 0.01$ and $y_0 = 10$, an exponential fit of the type $y = Ae^{Bx}$ gives $A = 10.1996(6)$ and $B = -0.00052496(2)$. Comparing with Eq. (10) we conclude that B corresponds roughly to the value of $-\delta$. The region expanded in Fig. 3(a) shows the passage of an orbit near a basin of attraction of the attracting fixed

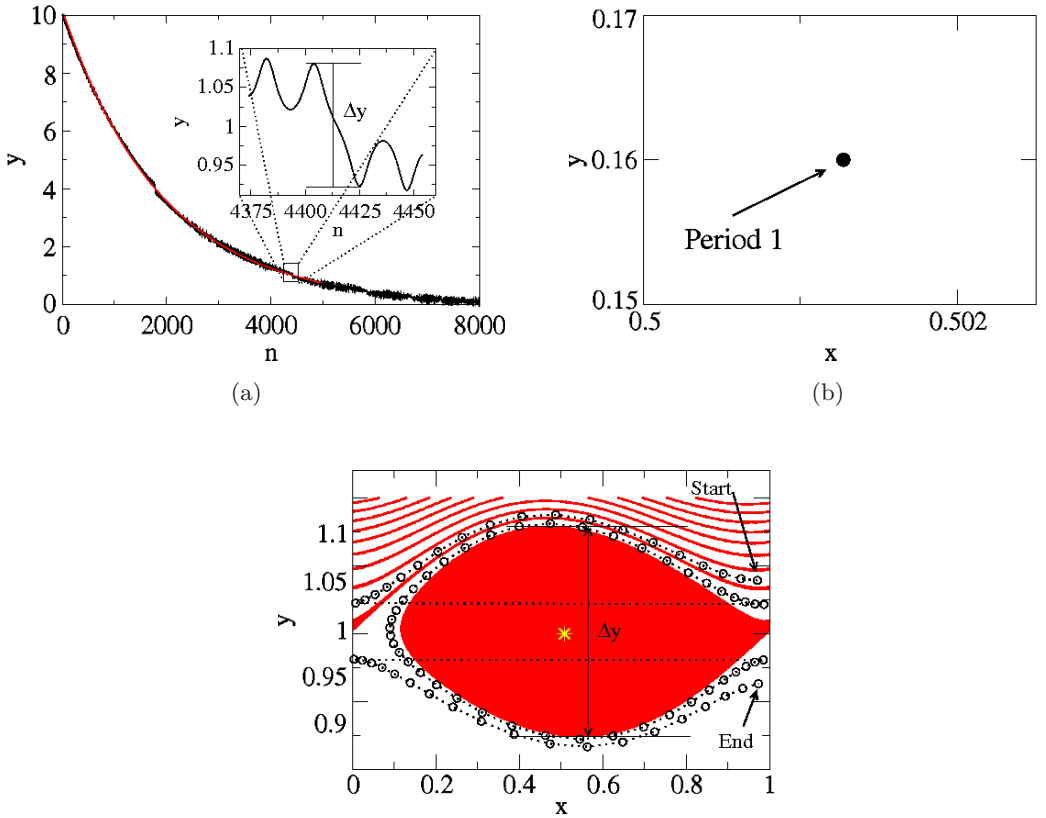

Fig. 3. (a) The behavior of y as a function of the number of iteration n. The initial condition used was $x_0 = 0.01$ and $y_0 = 10$. (b) Period-1 attracting fixed point (sink) and (c) $y \times x$. The control parameters used in both figures were $a = 2,\ b = 10^{-2}, \delta = 5 \times 10^{-4}$ and $\gamma = 1/2$.

point-sink (yellow star) as shown in Fig. 3(c). Figure 3(b) shows that evolving y as a function of n up to 10^7 iterations, the behavior of y decays exponentially for a period-1 attracting fixed point of coordinates $x = 0.5013$ and $y = 0.16$. Figure 3(c) shows the basin of attraction in red for a period-1 attracting fixed point (yellow star) and the evolution of an initial condition close to it. We see that the evolution of the initial condition around the basin of attraction starts at the initial condition in the arrow labeled Start and using circles connected by a dotted black line as a guide to the eye and ends in the arrow labeled End.

As the orbit approaches the fixed point, the general decay is characterized by an exponential function, however there are small oscillations around the average value. When the orbit passes near a large region influenced by a period-1 fixed point, it suffers a large perturbation which can cause a swap of rotation along the decay. To illustrate such behavior, Fig. 3(c) shows the basin of attraction for a period-1 attracting fixed point for $m = 2$, $x = 0.508$ and $y = 1$. The width on the y-coordinate for the large region of the basin of attraction is represented as Δy in Fig. 3(c). When the orbit passes near this region, it suffers a switch of rotation, as can be seen in the inset of Fig. 3(a).

For small dissipation and specific ranges of control parameters, the number of attractors in the phase space can be quite large. As an attempt to estimate the number of attractors present in the model, we have performed several simulations considering different sets of initial conditions. Figure 4 shows a histogram of frequency for the period of the orbit against its appearance in the phase space. The control parameters used were $a = 2$, $b = 10^{-2}$ and $\delta = 10^{-3}$. It is important to emphasize that in Fig. 4(a) the control parameter used was $\gamma = 1/2$ while in Fig. 4(b) was $\gamma = 3/4$. The number of initial conditions considered were 10^4, 9×10^4 and 2.5×10^5 uniformly chosen along the phase space. Each initial condition evolved 10^7 iterations, thus avoiding transient effects. For 10^4 initial conditions, it can be seen that low periodic attractors with

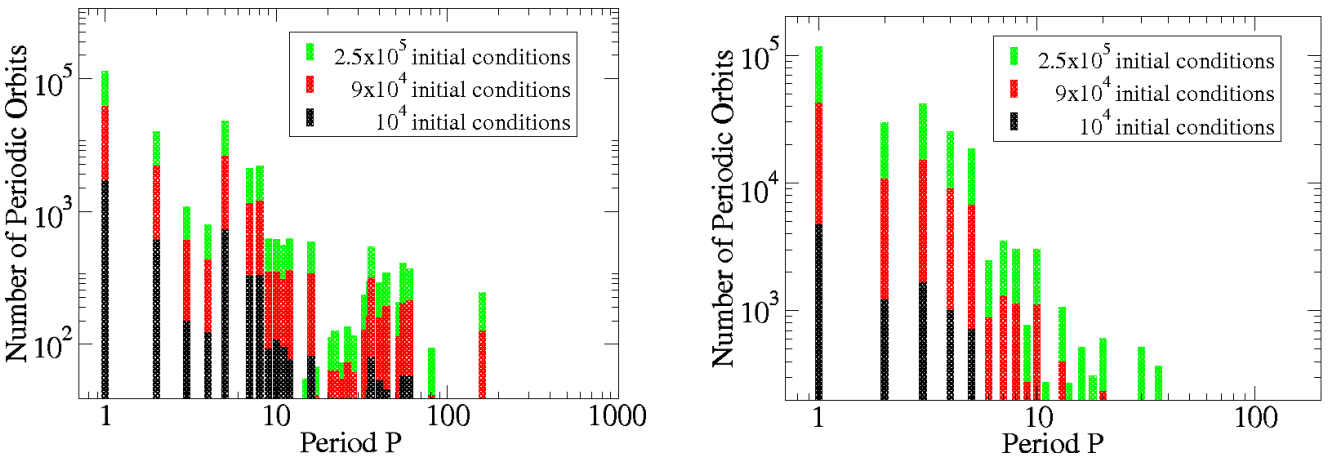

Fig. 4. Number of periodic orbits and their period using $a = 2, b = 10^{-2}$, $\delta = 10^{-3}$, (a) $\gamma = 1/2$ and (b) $\gamma = 3/4$.

period lower than 10 dominate over high periods, while, high periods are rarely found. It is important to note that the number of attractors obtained depends on the number of initial conditions used. For 10^4 initial conditions, the greater periodic orbit found for $\gamma = 1/2$ was 160, while for $\gamma = 3/4$ was 168. For 9×10^4 initial conditions, the largest periodic orbit observed for $\gamma = 1/2$ was 504 while for

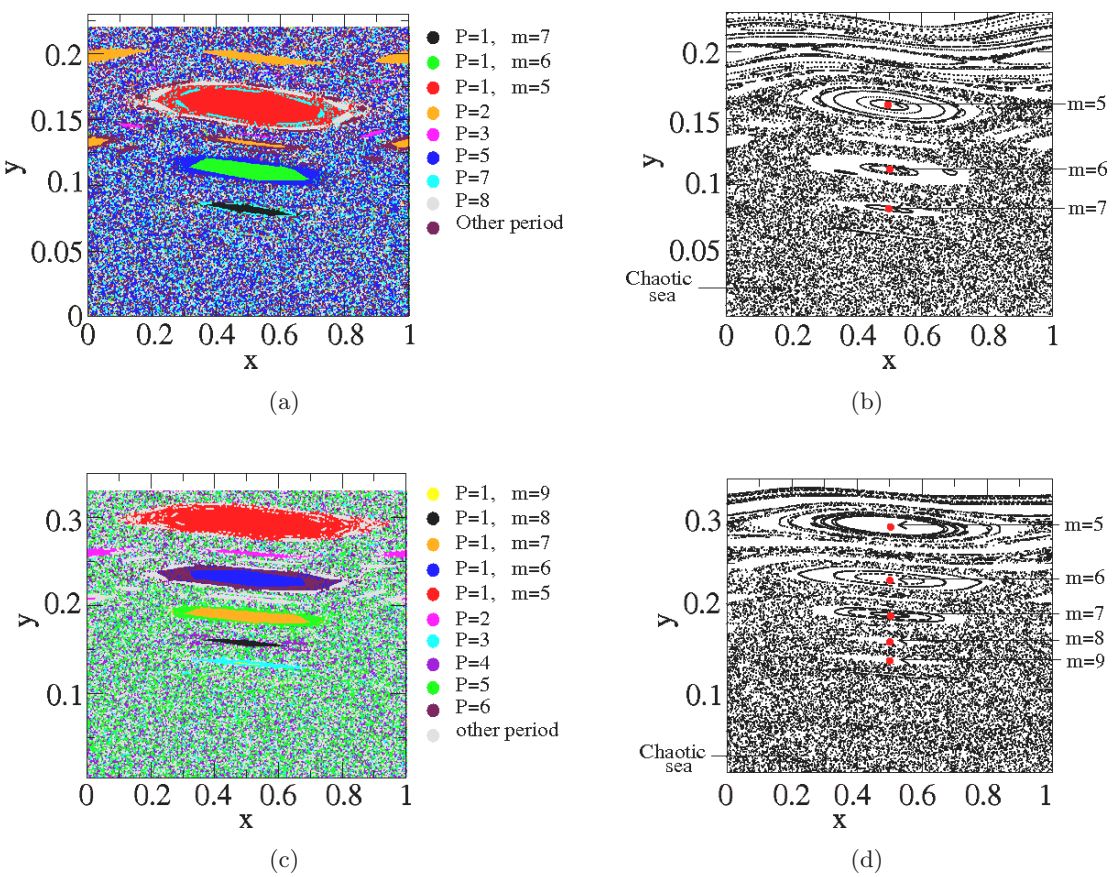

Fig. 5. (a) and (c) The basin of attraction for the periodic attractors shown in Fig. 1 for $\delta = 10^{-3}$. (b) and (d) The phase space for the nondissipative case respectively. The parameters used were $a = 2$, $b = 10^{-2}$, and (a) and (b) $\gamma = 1/2$; (c) and (d) $\gamma = 3/4$.

$\gamma = 3/4$ was 168. Finally for 2.5×10^5 initial conditions, the highest periodic orbit found for $\gamma = 1/2$ was 504 while for $\gamma = 3/4$ was 180. Applications of this procedure has also been discussed for a mechanical rotor model and Fermi–Ulam model [Feudel *et al.*, 1996; Tavares & Leonel, 2008].

Let us now comment on the basin of attraction for the attractors and the phase space for the nondissipative system. Figure 5 shows the basins of attraction for the fixed points shown in Fig. 1 with the corresponding phase space constructed for the nondissipative system. It can be seen that the largest basin of attraction shown in red in Figs. 5(a)–5(c) corresponds to the main orbit of period 1 ($P1$) of the phase space for the nondissipative system shown respectively in the Figs. 5(b)–5(d). The fixed points of the nondissipative system can be obtained by matching the following conditions: $y_{n+1} = y_n = y$ and $x_{n+1} = x_n = x + m$, where $m = 1, 2, 3, \ldots$. The (red) circle bullets in Figs. 5(b)–5(d) indicate the location of some of the elliptic fixed points, each one of them enumerated by m. A complete discussion of the fixed points for the nondissipative system as well as their classification was done in [de Oliveira *et al.*, 2010]. We can use the numeration of m to compare the basin of attraction with the phase space of the nondissipative system. In general, all basins of attraction of $P1$ orbits are relatively large when compared to those of the other period. To observe the basins of attraction for high periodic orbits, a large number of initial conditions is required. Figure 1 was constructed using 2.5×10^5 different initial conditions.

4. Conclusion

In this manuscript we have studied the effects of weak dissipation in a two-dimensional mapping parametrized by a control parameter γ as a dynamical variable. We showed that the dissipation creates attractors in the system. Specifically we observed the existence of a large number of coexisting periodic attractors and classified their periods. We proved analytically and confirmed numerically for this system that an orbit approaching an attracting fixed point is characterized by an exponential function. The number of periodic attractors was estimated and the structure of the basins of attraction was shown to be quite complicated. The phase space for the nondissipative system was used to compare the corresponding basin of attraction for the attracting fixed points in the dissipative case. We verified that all basins of attraction of period-1 ($P1$) orbits are relatively large when compared to those of other periods. Moreover, they correspond to large period-1 KAM islands on the conservative case. The present procedure can be applicable to many other different systems where a transition from conservative to weak dissipation is observed.

Acknowledgments

J. A. de Oliveira thanks CNPq and PROPe. E. D. Leonel kindly acknowledges the financial support from CNPq, FAPESP and FUNDUNESP, Brazilian agencies. The authors kindly acknowledge Prof. Dr. Denis G. Ladeira and Prof. Dr. Emanuel de Lima for a careful reading of the manuscript.

References

Berry, M. V. [1981] "Regularity and chaos in classical mechanics, illustrated by three deformations of a circular 'billiard'," *Eur. J. Phys.* **2**, 91.

Castro Neto, A. H. & Caldeira, A. O. [1991] "New model for dissipation in quantum mechanics," *Phys. Rev. Lett.* **67**, 1960.

de Oliveira, J. A., Bizão, R. A. & Leonel, E. D. [2010] "Finding critical exponents for two-dimensional Hamiltonian maps," *Phys. Rev. E* **81**, 046212.

Feudel, U., Grebogi, C., Hunt, B. R. & Yorke, J. A. [1996] "A map with more than 100 coexisting low-period periodic attractors," *Phys. Rev. E* **54**, 71.

Feudel, U. & Grebogi, C. [1997] "Multistability and the control of complexity," *Chaos* **7**, 4.

Feudel, U., Grebogi, C., Poon, L. & Yorke, J. A. [1998] "Dynamical properties of a simple mechanical system with a large number of coexisting periodic attractors," *Chaos Solit. Fract.* **9**, 171.

Howard, J. E., Lichtenberg, A. J., Lieberman, M. A. & Cohen, R. H. [1986] "Four-dimensional mapping model for two-frequency electron cyclotron resonance heating," *Physica D* **20**, 259.

Karlis, A. K., Papachristou, P. K., Diakonos, F. K., Constantoudis, V. & Schmelcher, P. [2006] "Hyperacceleration in a stochastic Fermi–Ulam model," *Phys. Rev. Lett.* **97**, 194102.

Ladeira, D. G. & Leonel, E. D. [2010] "Competition between suppression and production of Fermi acceleration," *Phys. Rev. E* **81**, 036216.

Leonel, E. D., McClintock, P. V. E. & da Silva, J. K. L. [2004] "Fermi–Ulam accelerator model under scaling analysis," *Phys. Rev. Lett.* **93**, 014101.

Leonel, E. D. & McClintock, P. V. E. [2006] "Effect of a frictional force on the Fermi–Ulam model," *J. Phys. A* **39**, 11399.

Leonel, E. D. [2007] "Corrugated waveguide under scaling investigation," *Phys. Rev. Lett.* **98**, 114102.

Leonel, E. D. & Tavares, D. F. [2007] "Consequences of quadratic frictional force on the one dimensional bouncing ball model," *Nonequilibrium Statistical Mechanics and Nonlinear Physics* **CP913**, 108.

Leonel, E. D. & Bunimovich, L. A. [2010] "Suppressing Fermi acceleration in a driven elliptical billiard," *Phys. Rev. Lett.* **104**, 224101.

Liberman, M. A. & Tsang, K. Y. [1985] "Transient chaos in dissipatively perturbed, near-integrable Hamiltonian systems," *Phys. Rev. Lett.* **55**, 908.

Lichtenberg, A. J. & Lieberman, M. A. [1992] *Regular and Chaotic Dynamics*, Appl. Math. Sci., Vol. 38 (Springer-Verlag, NY).

Luck, J. M. & Mehta, A. [1993] "Bouncing ball with a finite restitution: Chattering, locking, and chaos," *Phys. Rev. E* **48**, 3988.

Luna-Acosta, G. A., Na, K. & Reichl, L. E. [1996] "Band structure and quantum Poincaré sections of a classically chaotic quantum rippled channel," *Phys. Rev. E* **53**, 3271.

Luna-Acosta, G. A., Méndez-Bermudéz, J. A., Seba, P. & Pichugin, K. N. [2002] "Classical versus quantum structure of the scattering probability matrix: Chaotic waveguides," *Phys. Rev. E* **65**, 046605.

May, V. & Kuhn, O. [2000] *Charge and Energy Transfer Dynamics in Molecular Systems* (Wiley-VCH, Berlin).

Rabelo, A. F. & Leonel, E. D. [2008] "Finding invariant tori in the problem of a periodically corrugated waveguide," *Braz. J. Phys.* **38**, 54.

Rech, P. C., Beims, M. W. & Gallas, J. A. C. [2005] "Basin size evolution between dissipative and conservative limits," *Phys. Rev. E* **71**, 017202.

Rosa, J. & Beims, M. W. [2008] "Dissipation and transport dynamics in a ratchet coupled to a discrete bath," *Phys. Rev. E* **78**, 031126.

Saif, F., Bialynicki-Birulla, I., Fortunato, M. & Schleich, W. P. [1998] "Fermi accelerator in atom optics," *Phys. Rev. A* **58**, 4779–4783.

Saif, F. [2000] "Dynamical localization and signatures of classical phase space," *Phys. Lett. A* **274**, 98.

Seoane, J. M., Sanjuan, M. A. F. & Lai, Y.-C. [2007] "Fractal dimension in dissipative chaotic scattering," *Phys. Rev. E* **76**, 016208.

Smirnov, I. P., Virovlyansky, A. L. & Zaslavsky, G. M. [2001] "Theory and applications of ray chaos to underwater acoustics," *Phys. Rev. E* **64**, 036221.

Tavares, D. F. & Leonel, E. D. [2008] "A simplified Fermi accelerator model under quadratic frictional force," *Braz. J. Phys.* **38**, 58.

Tsang, K. Y. & Lieberman, M. A. [1984] "Analytical calculation of invariant distributions on strange attractors," *Physica D* **11**, 147.

Virovlyansky, A. L. & Zaslavsky, G. M. [2000] "Evaluation of the smoothed interference pattern under conditions of ray chaos," *Chaos* **10**, 211.

Zaslavsky, G. M. [1998] *Physics of Chaos in Hamiltonian Systems* (Imperial College Press, London).

Zaslavsky, G. M. [2002] "Chaos, fractional kinetics, and anomalous transport," *Phys. Rep.* **371**, 461.